



CENTER FOR INFRASTRUCTURE ENGINEERING STUDIES

Finite Element Modeling of Reinforced Concrete Bridge

Decks with ABAQUS

By

Ganesh Thiagarajan

Sujata Roy

**UTC
R111**

University Transportation Center Program at

The University of Missouri-Rolla

Disclaimer

The contents of this report reflect the views of the author(s), who are responsible for the facts and the accuracy of information presented herein. This document is disseminated under the sponsorship of the Department of Transportation, University Transportation Centers Program and the Center for Infrastructure Engineering Studies UTC program at the University of Missouri - Rolla, in the interest of information exchange. The U.S. Government and Center for Infrastructure Engineering Studies assumes no liability for the contents or use thereof.

Technical Report Documentation Page

1. Report No. UTC R111	2. Government Accession No.	3. Recipient's Catalog No.	
4. Title and Subtitle Finite Element Modeling of Reinforced Concrete Bridge Decks with ABAQUS		5. Report Date December 2005	
7. Author/s Ganesh Thiagarajan and Sujata Roy		6. Performing Organization Code 8. Performing Organization Report No. 00000768	
9. Performing Organization Name and Address Center for Infrastructure Engineering Studies/UTC program University of Missouri - Rolla 223 Engineering Research Lab Rolla, MO 65409		10. Work Unit No. (TRAIS)	11. Contract or Grant No. DTRS98-G-0021
12. Sponsoring Organization Name and Address U.S. Department of Transportation Research and Special Programs Administration 400 7th Street, SW Washington, DC 20590-0001		13. Type of Report and Period Covered Final	
15. Supplementary Notes		14. Sponsoring Agency Code	
16. Abstract The finite element method is still a predominant technique for the analysis of RC structures and can be a very effective tool to offset expensive experimental techniques. One commercially available finite element code, ABAQUS, has the unique ability to model the nonlinear behavior of concrete and steel as independent entities. This project will establish the methodology of modeling a typical RC bridge deck using ABAQUS and predict displacements, strains and stresses under normal traffic loads.			
17. Key Words Finite elements, RC bridge decks, ABAQUS, non-linear behavior modeling	18. Distribution Statement No restrictions. This document is available to the public through the National Technical Information Service, Springfield, Virginia 22161.		
19. Security Classification (of this report) unclassified	20. Security Classification (of this page) unclassified	21. No. Of Pages	22. Price

ABSTRACT

A bridge approach slab serves as a structural slab between the bridge structure and the approach embankment. The primary causes of approach slab failures are undermining, settlement and cracking. Undermining and settlement of the slab can be treated by either mud jacking or by pumping grout material to fill the voids beneath the slab. Transverse and longitudinal cracking leads to distress of the slab and reduces its life expectancy. The objective of this paper is to numerically study the extent and location of cracks by performing a non-linear finite element analysis of the slab. The factors affecting the cracks such as the thickness of the slab and the contact conditions with the soil underneath have been parametrically studied. This paper brings out the issues and advantages related to the usage of finite element analysis for approach slabs. The critical component of tension stiffening, has been calibrated before being used for the approach slab model. A thicker approach slab could be a more viable solution as compared to the expensive soil treatment.

Keywords: Bridge approach slab, parametric study, finite element analysis

1. INTRODUCTION

The riding discomfort, faced in everyday commute whenever one drives onto and away from the bridge is a ‘traveling-sore’ on the highway infrastructure system. An analysis of this situation will bring to light one of the noticeable causes of the discomfort, namely the “bump” at the end of the bridge. The “bump” is a complex problem and involves a number of components as stated in Briaud *et al.* [1997]. Some of the components are the natural soil on which the embankment is built, the approach slab, abutment type, approach fill material and the bridge/roadway joints. The important element of Briaud’s [1997] synthesis was the development of a “best current practice” list based on a survey of state DOT personnel namely, (a) treat the bump as a stand-alone design issue and prevention as a design goal, (b) assign the responsibility of this design problem to an engineer, (c) stress teamwork and open mindedness among the geotechnical, structural, pavements, construction, and maintenance engineers and (d) carry out proper settlement vs. time calculation, if differential settlement is excessive. The following situations were reported by Briaud *et al.* [1997] to minimize settlement a) a concrete approach slab of sufficient design, b) abutment and embankment on strong soil, c) well-compacted or stabilized fills, d) appropriate fill material (to provide strength and resist erosion), e) effective drainage, f) low embankments and g) good construction methods and inspection.

The performance of the approach slab is affected by geotechnical and structural factors. The geotechnical factors affecting performance are settlement of the approach fill

material, compression of the embankment fill material due to inadequate compaction, poor drainage, erosion of the fill material etc. The structural factors include the slab thickness, rebar areas and the soil-structure interaction characteristics.

Approach slabs also have structural cracking which reduces their life expectancy and their repair and replacement is a major financial burden to the transportation department. Cracks underneath the slab are hard to locate and repair. The problem not only affects the user but also over a period of time deteriorates the infrastructure of the country. As of 1995, there were 600,000 bridges across United States. Of these, 150,000 had problems with bumps at bridge ends, resulting in estimated expenditures of \$100 million per year to remedy the problem (Briaud *et al.*, 1997). Using these totals, the national average would calculate to nearly \$700 per year per bridge.

Detailed structural analysis of the bridge approach slab has been done in this paper using the nonlinear finite element program, ABAQUS. ABAQUS has the capability of modeling nonlinear behavior of concrete and steel. In addition it is also capable of treating steel as a separate input entity, allowing it to be modeled independently of concrete elements. This paper will help establish the potential of finite element analysis to provide dependable results of reinforced concrete structures and thus help reduce expensive laboratory experiments.

2. LITERATURE REVIEW

Finite element methods have been used for structural analysis purposes for a long time. For materials like concrete where discrete cracking occurs the constitutive behavior

is not that straightforward. A comprehensive summary by Darwin, [1993] gives a wide range of options available to perform an accurate analysis. It concludes that there are both usefulness and limitations of finite element modeling of reinforced concrete. “Smearred” cracking, properly handled, can adequately represent cracking in concrete. The “smearred” cracking representation should include either a tension stiffening or tension softening representation. Shear stiffness should be retained following cracking. The details of bond-slip between concrete and steel are, in most cases, of limited importance. There are some details of mesh dependency that must be considered. Biggs *et al.* [2000] evaluated the plausibility of finite element analysis of reinforced-concrete bridge decks using ABAQUS. They concluded that ABAQUS can model concrete and steel with beam and shell elements and can simulate their interaction. It can also calculate accurate results and predict behavior that cannot be generally be obtained through experimentation.

All studies of reinforced concrete employ one of the three possible strategies for representing the reinforcing steel: smearred, embedded, or discrete. Kwak and Filippou [1997] proposed a new smearred finite element model and a new reinforcing steel model, which is embedded inside a concrete element, but accounts for the effect of bond-slip. They concluded that a) the inclusion of tension stiffening is important for the independence of the analytical results from the size of the finite element mesh, but also for avoiding numerical problems in connection with crack formation and propagation, b) the effect of bond-slip is very important in the analysis of RC beams and beam-column assemblages even under monotonic loads and c) tension stiffening and bond slip cause opposite effects on the response of RC members.

Hoppe [1999] conducted a literature review regarding issues on the use, design and construction of approach slabs. The researcher mentioned that the presence of an approach slab has no effect on the magnitude of the differential settlement developed. There is no national consensus as to the real benefits or drawbacks of approach slab usage. The survey of most of the DOT's about the use, design and construction of the approach slab revealed that virtually every DOT has a unique set of criteria governing the use, design and construction of bridge approach slabs. Currently, there are no commonly accepted standards for evaluating the effectiveness of approach slabs and no unified policy for their selection. A common trend is to use approach slabs on roads with high volumes of traffic, typically on an interstate and primary systems. Beyond that, use guidelines, design methodology, material specifications, and construction techniques differ greatly from state to state. Survey responses indicate that a majority of state DOT's around the country consider bridge approach slab settlement as a serious and persistent maintenance problem. Settlement and the resulting bump at the end of the bridge should be viewed as a problem that requires engineering analysis on a site-specific basis to produce a cost effective solution. Approach fills should be considered structural elements, directly affecting performance of the adjoining bridge.

During the 1990's Missouri Department of Transportation (MoDOT) built more bridges than 47 other states [Luna *et al.*2003]. Significant percentage of these bridges have experienced settlement of their approaches. In some cases these slabs have even cracked near the abutment or experienced excessive settlement at the sleeper slab

producing a dip at that location. The current design of these bridge approach slabs includes provisions for the pumping of these slabs as a remedial measure.

Luna *et al.* [2003] carried out a detailed subsurface investigation to understand the deformation mechanisms. They recommended a reinforced soil embankment as a solution for the embankments that are of significant height. The reinforcement should be extended from the abutment a significant distance into the embankment. Compressibility of the foundation soils should be evaluated on a case-by-case basis based on additional boreholes completed before design behind the bridge abutment.

Cai *et al.* [2005] investigated the effect of embankment settlements on the performance of the approach slab. A 3-D finite element analysis was conducted considering the interaction between the approach slab and the embankment soil, and consequently the separation of the slab and soil. The predicted internal moments of the approach slab provide design engineers with a scientific basis to properly design the approach slab considering different levels of embankment settlements. Current American Association of State Highway Transportation Officials (AASHTO) code specifications do not provide clear guidelines to design approach slabs considering the embankment settlements.

Some slab-on-grade problems were also investigated as a slab-on-grade behavior is affected by some of the factors, which affect the performance of approach slab. Al-Nasra *et al.* [1994] have done a finite element analysis of a slab-on-grade and have studied the effects of slab thickness, modulus of sub grade reaction, modulus of elasticity

of concrete etc. It was concluded that the cracking load increases with decrease in modulus of sub grade reaction.

Hani Nassif *et al.* [2002] investigated the cracking in bridge approach slab and transition slabs which have been persistent problems. The main objective of the study was to identify the probable causes of cracking, location of cracks, the factors affecting cracking and also to recommend design alternatives that reduce crack development in approach and transition slab. The outcome of the study showed that the thickness of the slab is the most effective parameter in reducing the tensile stress in the critical elements. It was also inferred that increasing the concrete compressive strength increases the cracking load capacity but is not very effective in comparison with an equivalent increase in the thickness of the slab. Increasing the steel reinforcement yielding stresses has no effect on either the cracking load capacity of the approach and transition slab or the stresses in the critical elements. Three new design alternatives were suggested for the design of the approach slab namely, a) the constant thickness design, b) deep beam design and c) embedded beam design.

In this paper the performance of the bridge approach slab with regard to void development and slab thickness, based on a non-linear analysis of approach slabs, has been presented. The cracking patterns for different cases of void development have been studied. The finite element modeling of the approach slab has been presented in section 4, the parametric study showing cracking of the slab and the factors affecting it has been presented in section 5 and the conclusions have been drawn in section 6.

3. ABAQUS MATERIAL MODEL

Three major effects cause the non-linear response of reinforced concrete namely, a) crushing in compression, b) cracking of concrete in tension and c) yielding of reinforcement. Nonlinearities also arise from the interaction of the constituents of reinforced concrete such as, bond-slip between reinforcing steel and surrounding concrete, aggregate interlock at a crack and dowel action of the reinforcing steel crossing a crack. Time dependent effects of creep, shrinkage and temperature variation also contribute to the non-linear behavior.

Smearred Crack Model for Concrete: The smeared crack model represents the discontinuous macro crack brittle behavior. In this approach individual macro cracks are not tracked, rather the presence of cracks enters into the calculations by the way the cracks affect the stress and material stiffness associated with each material calculation point. For simplicity, the term “crack” is used to mean a direction in which cracking has been detected at the material calculation point in question.

Reinforcement Model: Reinforced concrete modeling in ABAQUS is accomplished by combining standard elements, using the plain concrete model, with “rebar elements”—rods, defined singly or embedded in oriented surfaces, that use a one-dimensional strain theory and that may be used to model the reinforcing steel itself. These elements are superposed on the mesh of plain concrete elements and are used with standard metal plasticity models that describe the behavior of the rebar material. This modeling approach allows the concrete behavior to be considered independently of the rebar. Effects

associated with the rebar/concrete interface, such as bond slip and dowel action, cannot be considered in this approach except by modifying some aspects of the plain concrete behavior to mimic them (such as the use of “tension stiffening” to simulate load transfer across cracks through the rebar).

Tension Stiffening: The phenomenon of concrete to carry tension even after cracking is represented in a finite element model by the use of tension stiffening. The tension stiffening effect improves the accuracy of the finite element (FE) models in representing cracks and, in some cases, improves the numerical stability of the solution. The tension stiffening effect must be estimated; it depends on such factors as the density of reinforcement, the quality of the bond between the rebar and the concrete, the relative size of the concrete aggregate compared to the rebar diameter, and the mesh. A reasonable starting point for relatively heavily reinforced concrete modeled with a fairly detailed mesh is to assume that the strain softening after failure reduces the stress linearly to zero at a total strain of about 10 times the strain at failure. The strain at failure in standard concretes is typically 10^{-4} (ϵ_{cr}), which suggests that tension stiffening that reduces the stress to zero at a total strain of about 10^{-3} is reasonable. This parameter should be calibrated before usage in any model.

Shear Retention: As the concrete cracks, its shear stiffness is diminished. This option in ABAQUS defines the reduction of the shear modulus associated with crack surfaces in a concrete model as a function of the tensile strain across the crack.

3.1 McNeice Slab Study

To study the effects of tension stiffening on a reinforced concrete slab the McNeice [1967] slab is studied. Concrete stress-strain, steel stress-strain, load-deflection and the cracking behavior of the slab have been studied for different tension stiffening values [Roy, 2005].

Model Description: The model being analyzed here is a square slab supported at its four corners and loaded by a point load, 18.4kN at its center. The slab is reinforced in two directions at 75% of its depth. The reinforcement ratio (volume of steel/volume of concrete) is 8.5×10^{-3} in each direction. The slab spans 0.9 m either way and is 44.4 mm thick. Figure 1 show the slab plan and cross-section details. The slab was tested experimentally by McNeice [1967]. The material properties of concrete are taken from Gilbert and Warner [1978]. Some of these data are assumed values, because they are not available for the concrete used in the experiment. Four different values for the strain beyond failure at which all strength is lost; 5×10^{-4} ($5 \varepsilon_{cr}$), 1×10^{-3} ($10 \varepsilon_{cr}$), 2×10^{-3} ($20 \varepsilon_{cr}$) and 5×10^{-3} ($50 \varepsilon_{cr}$) are used to illustrate the effect of the tension stiffening parameter on the response. The concrete tensile stress and failure strain as used are shown in Figure 2.

Concrete Compressive Stress: Stress S_{11} for concrete (bottom surface - SNEG and top surface - SPOS) is plotted as histograms (figure 3) for all the integration points in element 1 and for each of the tension stiffening values. From the plot in figure 3 it can be

inferred that concrete behavior is most correctly represented when the tension stiffening value is 0.002. The histogram plot for the other tension stiffening values doesn't represent the concrete behavior within the tension regime.

Observations from Tension Stiffening Studies: The following observations were made from the preliminary tension stiffening studies, Roy [2005].

a) Concrete stresses for SPOS are always negative which agrees with the fact that the stresses are mostly compressive on the top surface of slab.

b) Concrete stresses for SNEG are not always tensile. The stress output for SNEG when compared with strain output for SNEG shows that the stress output for tension stiffening ($20 \varepsilon_{cr}$) agrees with the expected behavior. It can be concluded that tension stiffening values, somewhere in the middle should be chosen for the analysis. Lower values as well as higher values of tension stiffening did not predict the behavior accurately.

c) Rebar strains also have a tendency to increase with increasing tension stiffening values.

d) The deflection at each time step increases with increasing tension stiffening values. From the slope of the load deflection curve it can be inferred that the stiffness keeps decreasing as tension stiffening value is increased.

4. APPROACH SLAB MODEL

A typical approach slab configuration employed in bridge construction has the slab supported on the abutment back wall at one end and on the adjoining highway at the other. A typical MoDOT bridge approach slab arrangement has the slab supported at one end by the abutment and at the other by a sleeper beam resting on the embankment. The sleeper slab support is used, to equalize settlements beneath the roadway end of the approach slab.

Slab Geometry: The slab dimensions used in the finite element analysis are: length of 7.5 m., width of 3.6 m and thickness of 0.3 m. The model was divided into elements, each having a length of 254 mm x 183 mm based on a tire patch area size as specified by AASHTO. The four noded reduced integration shell element is used for the slab. The total number of nodes and elements in the model are 651 and 600 respectively. In order to model the contact between the slab and the soil, each of the inner nodes was attached to a spring element. The connection between the approach slab and bridge abutment as well as the sleeper beam sides are represented by pin connections.

Loading: The loading on the slab has been given as per AASHTO LRFD Bridge Design Specification. The design truck and design lane load has been applied. The loading has been applied in steps with the design truck entering the slab at the pavement end and then traversing the slab. The design lane load is always present on the slab along with the design truck load. The load has been applied as pressure loads on the top surface of the approach slab.

The pressure due to axle loads tire contact area as specified in AASHTO specifications has been used. The tire contact area of a wheel consisting of one or two

tires shall be assumed to be a single rectangle, whose width is 508 mm and whose length is 254 mm. The tire pressure is uniformly distributed over the contact area. The pressure load for the design truck was calculated for each of the axle loads. The wheel load of 17.7 kN (4 kips) had a pressure of 0.137 MPa (20 psi) and the wheel load of 70.8 kN had a pressure of 0.55 MPa. The design lane load has a uniform pressure of 0.003 MPa (0.46 psi) distributed uniformly over the entire length of the slab and over a span of 3.6 m (10 ft.) transversely.

Soil Structure Interaction: The soil stratum underneath the slab is represented by a series of linear elastic springs having constant stiffness. Four sets of spring stiffness values based on the contributory area of each node. The modulus of subgrade reaction is used for calculating the spring stiffness has been calculated. The modulus of subgrade reaction is a conceptual relationship between soil pressure and deflection that is widely used in the structural analysis of foundation members. A range of values for modulus of subgrade reactions is given in Bowles [1996] based on which a few soil types have been investigated for the approach slab model. The soil “spring” will have units of FL^{-1} (F=Force, L=Length) obtained from the modulus of subgrade reaction and the contributory node area. Four different values of modulus of subgrade reaction have been used for comparison corresponding to four different types of soil properties.

The first case was considered with a modulus of subgrade reaction (k_s) of 5000 kN/m^3 (18.4 lb/in^3) representing loose sand type of soil assuming full contact of the slab with the soil. The plot shown in figure 4 corresponds to symbol plot of plastic strain on the bottom surface (SNEG) of the slab. The cracks are transverse in nature and are spread

across the slab. The maximum displacement (U_3) observed is 14 mm. The deflection values are observed for the central part of the slab and helps in comparing the deflection numerically with the other cases that are presented in the following paragraphs.

It can be seen in figure 4 that the plastic strain plot at the center appears as a solid straight line while those at the edges appear discrete and inclined. It has been observed that when the cracks initiate the plastic strain plot is discrete in nature. For instance at the center the initiation of cracks started as discrete plots and as the truck wheel loads passed through and beyond they progressed to appear as solid lines. Hence, the discrete lines at the end of the slab can be interpreted as the initial stages of cracking. The final plot is indicative of the cracking throughout the entire span.

The second case was run with a modulus of subgrade reaction (k_s) of 25,000 kN/m^3 (92.1 lb/in^3) as considered by Hani Nassif [2002]. The soil type is silty medium dense sand. The plot shown in figure 5 is a plastic strain symbol plot for the final step (step 17) of the loading history. The crack patterns can be seen transverse to the direction of traffic movement. The maximum displacement (U_3) for this case is 3.3 mm.

The third case was considered with the modulus of subgrade reaction of 50,000 kN/m^3 . The type of soil can be clayey medium dense sand or can be medium dense sand. There are no cracked elements for this case. The displacement (U_3) is 1.73 mm.

Finally, the fourth case refers to a modulus of subgrade reaction of 107,000 kN/m^3 , as taken by Al Nasra [1994]. The type of soil is dense sand. There were no cracked elements for this case and the displacement (U_3) was 0.84 mm. Since the

results are more pronounced with the value of 5000 kN/m^3 , this value has been chosen for the subsequent parametric study.

Reinforcement stresses: The analysis of the approach slab when the design truck and the design lane load are present and all the spring elements activated, yielded low rebar stresses of the order of 41.4 MPa . These low stresses inspired the following trial to achieve rebar yield stresses. The worst combination of loads was considered when both the 142.3 kN axles are on the slab and the lane load is also present. All the spring elements were deactivated for the model and only the end boundary conditions are present. The rebar stresses for this case reached up to 172.4 MPa [Roy, 2005].

From various trials conducted by increasing the loads, it was concluded that the reinforcement provided in the approach slab is over designed and that the yield limit is mostly reached when the loading on the slab is more than double than that of a standard design truck. The input components for the parametric study of the approach slab were finalized from the above validation study.

5. PARAMETRIC STUDY

Parameters: Not much work has been reported on the interaction between approach slab and embankment settlement to investigate the approach slab performance. The factors affecting cracking of the slab are: a) concrete compressive strength, b) rebar cross-sectional area, c) rebar yield stress, d) thickness of slab and e) void development.

The yield stress of the rebar doesn't have much affect on the slab performance as seen from the validation studies, where it was observed that the rebar stresses are low and that they reach yield limits only when the loads are high. Hence, concrete compressive

strength and rebar yield stress were not considered as parameters for this study. As the rebar cross-sectional area provided in the MoDOT specification for a typical approach slab is considerably high, no attempt has been made in this work to consider that as a parameter to be changed and studied.

The slab thickness and development of voids beneath the slab are the major factors influencing the slab performance with regard to cracking. Hence, a parametric study of the slab has been done to analyze the effect of these two factors on slab cracking.

Slab Thickness: The maximum slab thickness in MoDOT specification for the bridge approach slab is 304.8 mm. A higher slab thickness of 355.6 mm was used for the parametric studies. The soil properties chosen for the parametric studies are the loose sand type with modulus of subgrade reaction of 5000kN/m^3 . All the springs were considered active for this analysis. The loading used were the standard design truck load (applied in steps) along with the design lane load. Since serviceability criteria of the slab is investigated only service loads have been considered for the parametric studies. An analysis has also been performed to demonstrate the effect of factored live loads on the approach slab.

Crack Pattern for Slab Thickness of 304.8 mm.: The plot for plastic strain is analyzed for the load step at which the cracking begins (load step 7) and also the final load step (load step 17) at which the truck load exits the slab. It is observed that the crack patterns are on the bottom surface (SNEG) of the slab. The corresponding deflection at load step 7 is 3.81 mm. and at load step 17 is 13.97 mm. From the plots it can be inferred that the

cracks are transverse in nature and are spread across the slab. Figure 6 is representative of plastic strain plot for load step 17.

Crack Pattern for Slab Thickness of 355.6 mm.: The slab parameters changed for this analysis include changing the slab thickness to 355.6 mm and also the reinforcement, based on the nominal moment capacity for slab with thickness 304.8 mm. It was observed [Figure 30, Roy, 2005] the load step 7 when cracking begins that the cracks are spread over four rows of elements as compared to 7 rows of elements for the case when thickness of slab is 304.8 mm, [Figure 28, Roy 2005]. The difference in the number of rows of cracked elements can also be seen for load step 17 as shown in figure 7. Table 1 shows the summary of the deflection at the final load step and also the number of the rows of cracked elements for slab thickness of 304.8 mm and 355.6 mm.

Void Modeling: Voids develop beneath the approach slab between the slab and the soil and affects the structural performance of the slab. Voids mostly develop at the interface between the abutment and the slab. This area is more prone to the development of voids since it is hard to achieve the desired compaction of the soil in this region. This happens because the abutment is constructed before the approach embankment and hence it is difficult to physically reach that area for compaction.

In this study, voids have been considered up to 0.91 m., 1.83 m., and 2.74 m. from the abutment end. To idealize the voids springs elements have been removed from nodes till 0.91 m, 1.83 m. and 2.74 m. from the abutment end. Comparison of the cracking patterns observed and the deflection for the final load step has been presented for both slab

thickness of 304.8 mm. and 355.6 mm. The modulus of subgrade reaction has been kept at 5000 kN/m³.

For the 304.8 mm. thick slab two more cases have been considered. The first one is when voids develop fully underneath the slab and the other case is when factored loads are considered for the design loading on the slab.

Voids up to 0.91 m.: Crack patterns corresponding to the final load step has been shown in figures 8 and 9 for the 304.8 mm. and 355.6 mm. thick slab respectively. The plots are symbol plot and are for the SNEG face (bottom) of the slab. Table 2 gives the deflection and the number of cracked element rows observed for each of the slab thickness.

Voids up to 1.83 m.: Crack patterns corresponding to the final load step has been shown in figures 10 and 11 for the 304.8 mm. and 355.6 mm. thick slab respectively. The plots are symbol plot and are for the SNEG face (bottom) of the slab. There are no crack patterns observed for the SPOS (top) face of the slab. Table 3 gives the deflection and the number of cracked element rows observed for each of the slab thickness. It can be seen from Table 3 that the number of cracked element rows are the same as for the case of voids till 0.91 m.

Voids up to 2.74 m.: There are no crack patterns observed for the SPOS (top) face of the slab. The deflection observed for this load step is 4.57 mm. The deflection for this step is 18.8 mm. It has also been observed that there is not much difference in the plastic strain plot for the case when voids are up to 1.83 m. and when voids are up to 2.74 m. [Roy, 2005] Hence, for the 355.6 mm. slab this comparison has not been performed.

Voids on Entire Slab: This case has been analyzed for the worst-case scenario when the approach slab loses contact with the soil completely. The analysis run exited early and the error generated is a diverging solution. From the plastic strain plot for the last load step for the top surface of the slab [Figure 42, Roy 2005], it is observed that both the longitudinal and transverse cracking is seen on the top surface of the slab. The deflection for the final load step is 166.62 mm. and the rebar stresses reach their yield limit of 344.74 MPa for this case.

Factored Load on Slab: Load factors have been applied on the live load based on AASHTO specification. The slab is considered to be fully in contact with the soil. The cracks on the top of slab are approximately at 2.44 m. from the abutment/slab interface. The nature of the cracks is transverse and they tend to spread across the slab. The deflection at final load step is 31.75 mm.

5.1 Observations from Parametric Studies

The parameters studied considered were the thickness of the bridge approach slab and development of voids beneath the slab. Due to the change in thickness, the deflection at the central portion of the slab, at the final load step is less for the case of 355.6 mm. (thicker) slab. Since the ends of the slab are pinned and have no deflection, there is a gradient change from the center of the slab to the end of slab at the slab/bridge interface. This situation also actuates the “bump” at the slab/bridge interface, which indicates that deflection control (serviceability constraint) should be an important consideration in the design of approach slabs. The deflection values are also higher for the case when the voids beneath the slab are increased.

The crack patterns observed show lesser number of rows of cracked elements when the thickness of the slab is increased. For the cases when voids are up to 0.91 m. and up to 1.83 m. from the abutment end, the numbers of rows of cracked elements are the same. However, the difference lies in the intensity and also the extent of the cracks, which is greater for the 1.83 m. void case. The crack patterns are mostly observed in the bottom surface of the slab. Cracks on the top of slab are seen when factored loads are applied to the slab.

It is seen from this study that both the parameters significantly affect the deflection and cracking behavior and hence the life span of the bridge approach slab. Excessive deflection of the slab causes riding discomfort and the cracks on the bottom of the slab are difficult to locate and repair. Cracks on top of slab make the slab more prone to harmful effects of deicing salts.

6. CONCLUSIONS

The following conclusions can be drawn from the performance-based study of the bridge approach slab using nonlinear finite element methods:

- ABAQUS models reinforced concrete behavior well and can be used for analysis of other reinforced concrete structures where the stress/strain behavior and deflections are critical components.
- For the finite element model tension stiffening must be added, to model the interaction behavior of concrete and steel in the post cracked stage. The tension

stiffening value must be estimated before performing an analysis. For this study a value of $20\epsilon_{cr}$ was found suitable.

- Concrete compressive strength and rebar yield stress were not considered as parameters, in this study, affecting the approach slab performance. The reason they were not considered was that using very high strength concretes may not be feasible in the entire scheme of bridge construction and that the yield stress for the rebars is reached only for high (ultimate) loads on the slab. For the MoDOT bridge approach slab the rebar stresses were found to be much lower than their yield limits, from which it can be inferred that the steel provided is over designed, from a strength consideration.
- The slab behavior as the voids under the slab increases shows an increase in transverse cracks at the abutment/approach slab interface. The deflection of the slab also increases with the increasing voids.
- The number of rows of cracked elements is the same for the case of voids up to 0.91 m. and 1.83 m., but the intensity of cracks are different. The cracks are denser and are spread over more elements for the 1.83 m. void situation as compared to the 0.91 m. case.

Acknowledgements

The authors would like to acknowledge Professor A. Nanni, Director of the University Transportation Center, Rolla for partially funding this study and Dr. Bryan Hartnagel and Mr. Thomas Fennessey of Missouri Department of Transportation (MoDOT) for useful discussions related to this study.

References

1. AASHTO LRFD Bridge Design Manual, 1998.
2. Al-Nasra Moayyad, Wang R. L. Leon (March-April, 1994), *Parametric Study of Slab-on-Grade Problems due to Initial Warping and Point Loads*, ACI Structural Journal, Vol. 91 no 1, pp. 198-210.
3. Biggs R. Michael, Furman W. Barton, Jose P. Gomez, Peter J. Massarelli and Wallace T. McKeel, (September, 2000). *Finite Element Modeling and Analysis of Reinforced-Concrete Bridge Decks*, Virginia Transportation Research Council, Final Report.
4. Bowles, Joseph E. (1996). *Foundation Analysis and Design*. Fifth Edition, McGraw-Hill Companies, Inc., New York.
5. Briaud, Jean-Louis, James, Ray W. and Hoffman, Stacey B. (1997), *Settlement of Bridge Approaches "Bump at the end of the Bridge"*, TRB, NCHRP Synthesis of Highway Practice 234, National Academy Press, Washington, D.C.
6. Darwin, D. (1993). *Reinforced Concrete*. In *Finite Element Analysis of Reinforced-Concrete Structures II: Proceedings of the International Workshop*. New York: American Society of Civil Engineers, pp. 203-232.
7. Gilbert, R. I. and R.F Warner, (1978), *Tension Stiffening in Reinforced Concrete Slab*, Journal of the Structural Division, American Society of Civil Engineers, Vol. 104, ST12, pp. 1885-1900.
8. Hani Nassif, Talat Abu-Amra, Nirali Shah, (2002). *Finite Element Modeling of Bridge Approach Slab and Transition Slab*, FHWA NJ 2002-007, Final Report.
9. Hibbit, Karlsson and Sorenson, Inc. (1998). *ABAQUS/ Standard User's Manual; Version 6.1 (Vols. I-III)*
10. Hibbit, Karlsson and Sorenson, Inc. (1998). *ABAQUS/ Standard Update Manual; Example Problems, Verification, Theory; Version 6.1*
11. Hoppe, J. Edward, (1999), *Guidelines for the Use, Design, and Construction of Bridge Approach Slabs*. Virginia Department of Transportation and the University of Virginia, Final Report.
12. Kwak, H.G. and Filippou, F. C. (1997). *Nonlinear FE Analysis of Reinforced Concrete Structures under Monotonic Loads*. Computers and Structures, 65(4): pp.585-592.
13. Luna, Ronaldo, Robison, J. L, Wilding, Andrew (2003). *Evaluation of Bridge Approach Slabs, Performance and Design*. University Transportation Center Program at University of Missouri Rolla, Final Report.
14. McNeice (1967). Collapse of a Concrete Slab. *ABAQUS Examples Manual Version 6.1*.
15. Roy Sujata (2005). *Nonlinear Finite Element Analysis of Reinforced Concrete Bridge Deck/Bridge Approach Slab Using ABAQUS*, M.S. Thesis in Civil Engineering at University of Missouri Kansas City.
16. Cai C. S., Shi, X. M., Voyiadjis, G. Z. and Zhang Z. J. (July, 2005), *Structural Performance of Bridge Approach Slabs under Given Embankment Settlement*, ASCE Journal of Bridge Engineering, Vol. 10, No. 4pp 482-489.

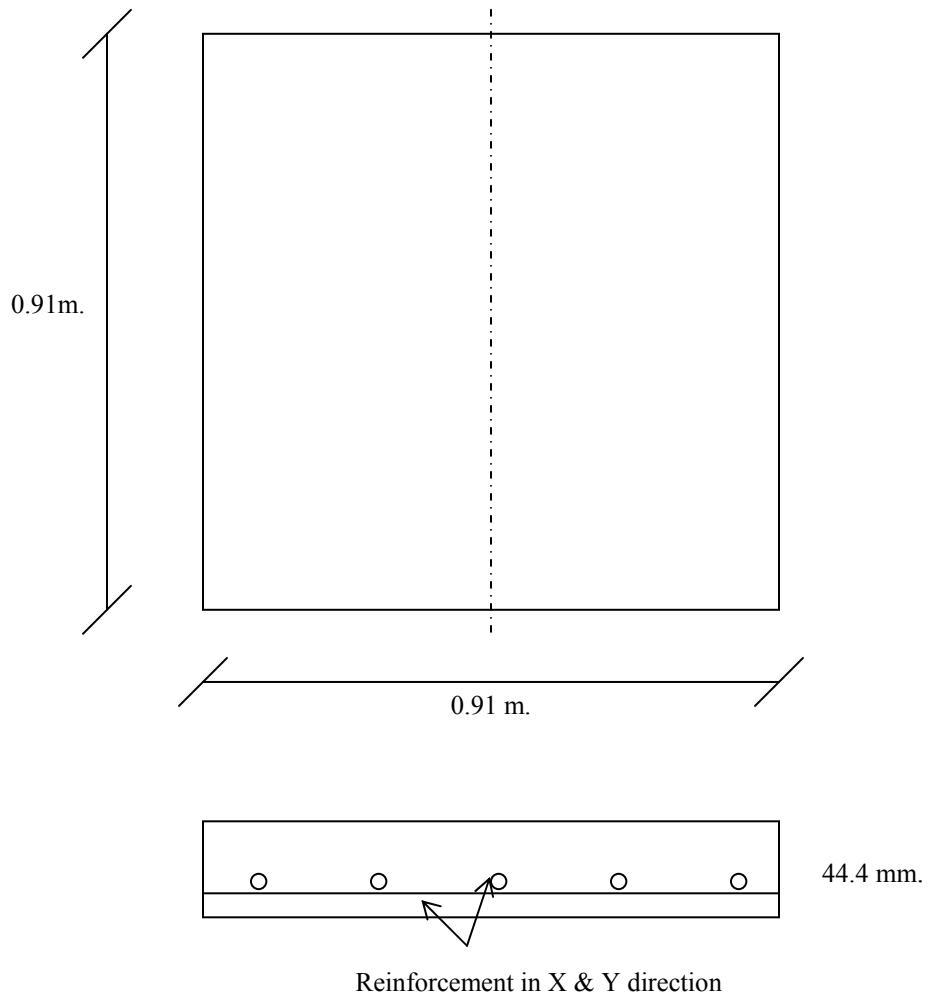


Figure 1: McNeice Slab Used for the Study

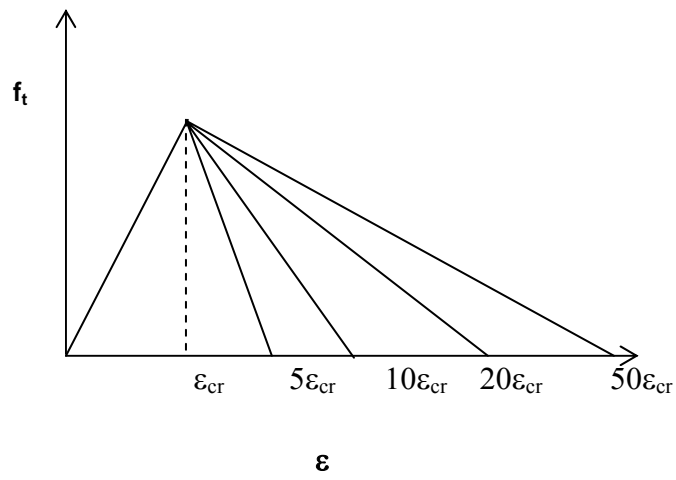


Figure 2 Tension Stiffening vs. Concrete Tensile Strain

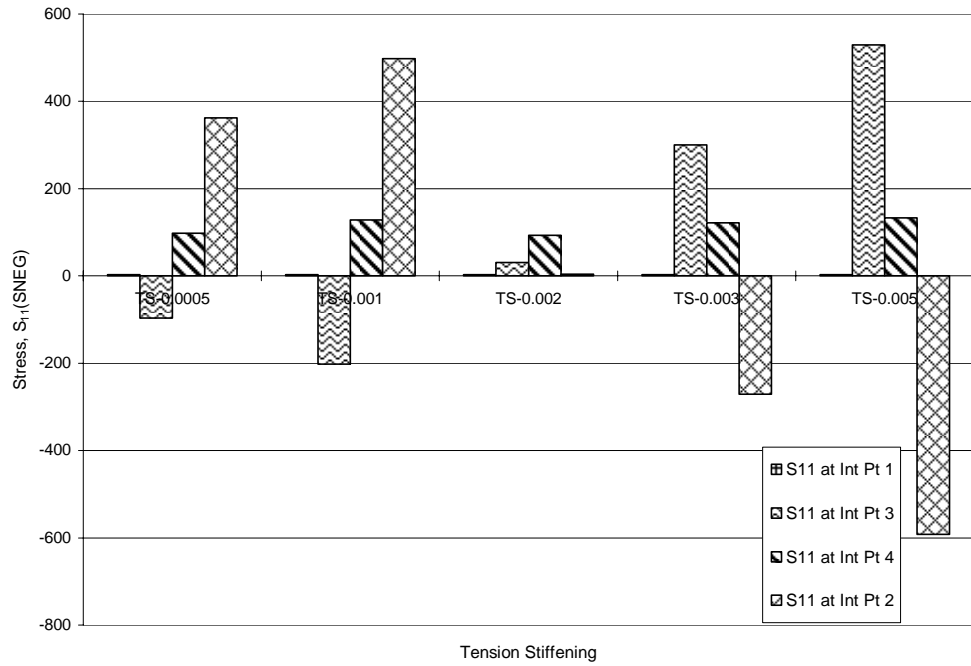


Figure 3: Histogram of Concrete Tensile Stress for Element 1 and Tension Stiffening

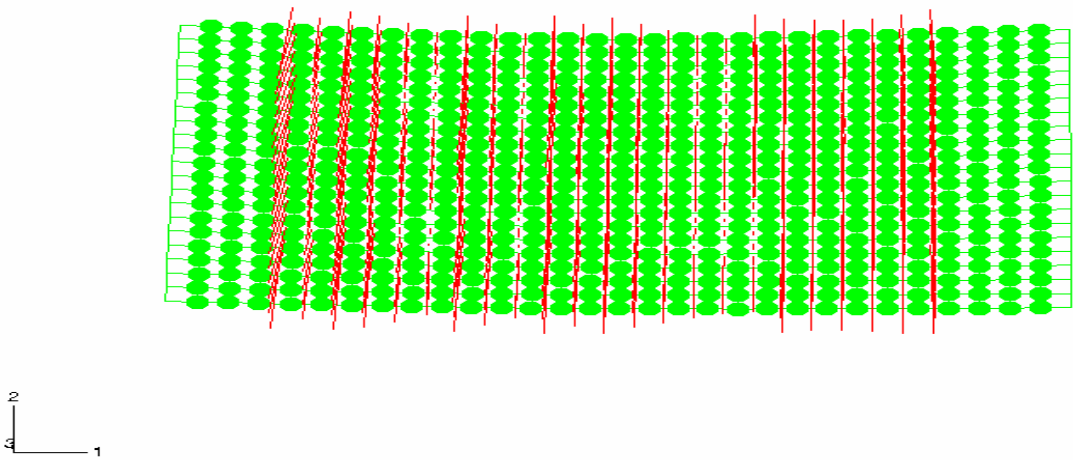


Figure 4 Crack Pattern, SNEG for, Load Step 17, $k_s= 5000\text{kN/m}^3$

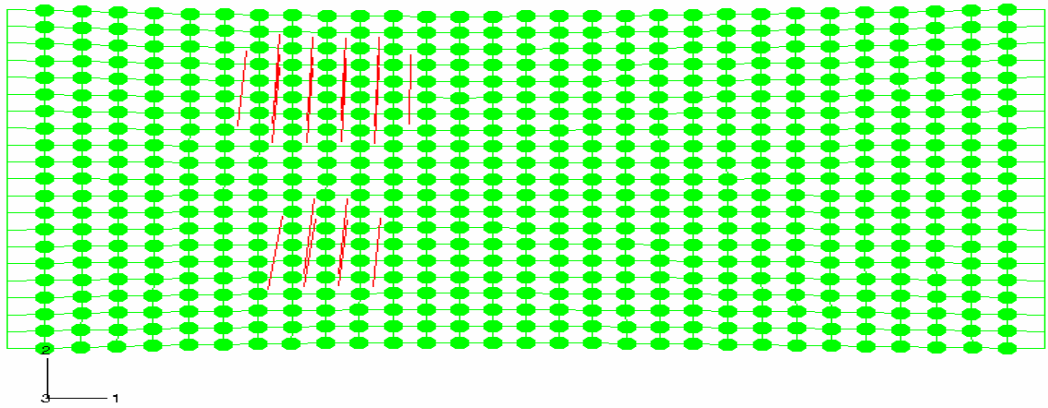


Figure 5. Crack Pattern for, SNEG, Load Step 17, $k_s=25000\text{kN/m}^3$

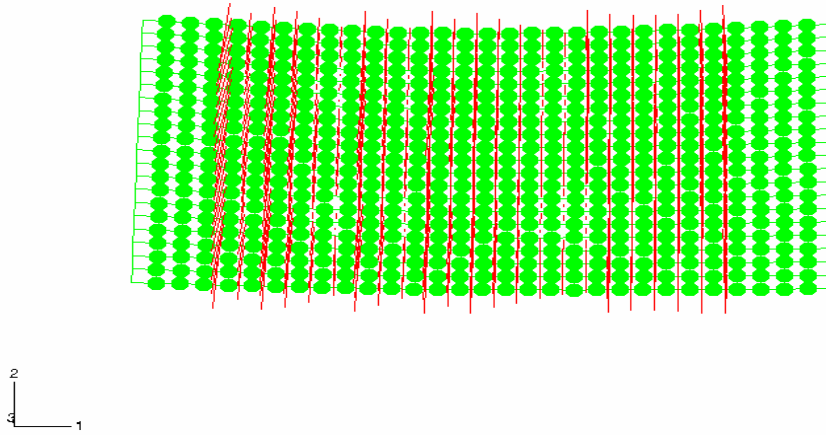


Figure 6. Crack Pattern for SNEG, Load Step 17, Slab Thickness 304.8 mm.

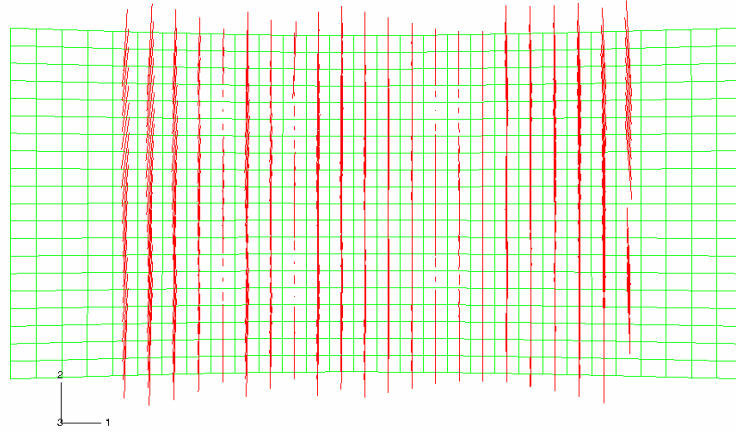


Figure 7 Crack Pattern for SNEG, Load Step 17, Slab Thickness 355.6 mm.

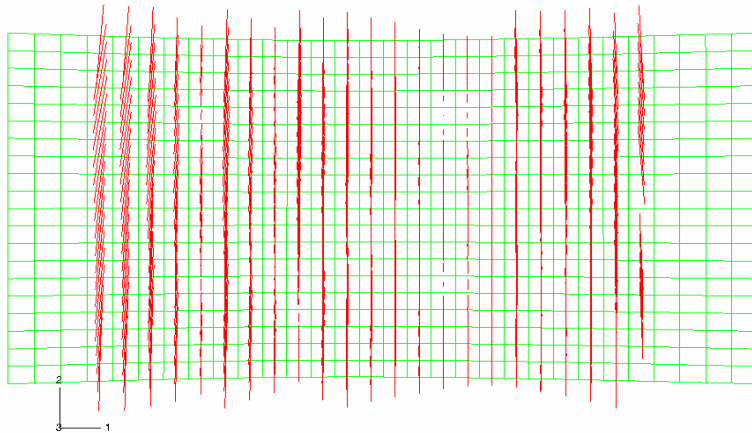


Figure 8 Crack Pattern for SNEG, Load Step 17, Slab 304.8 mm., Voids 0.91 m.

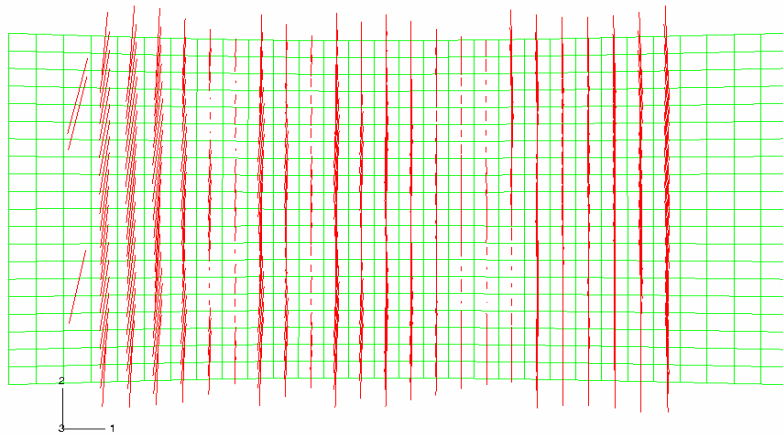


Figure9: Crack Pattern for, SNEG, Load Step 17, Slab 355.6 mm., Voids 0.91 m.

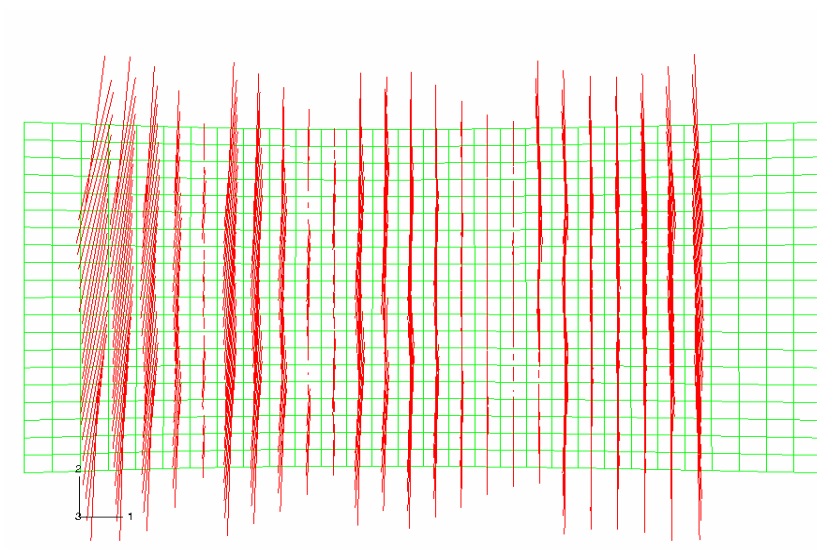


Figure 10: Crack Pattern for, SNEG, Load Step 17, Slab 304.8 mm., Voids 1.83 m.

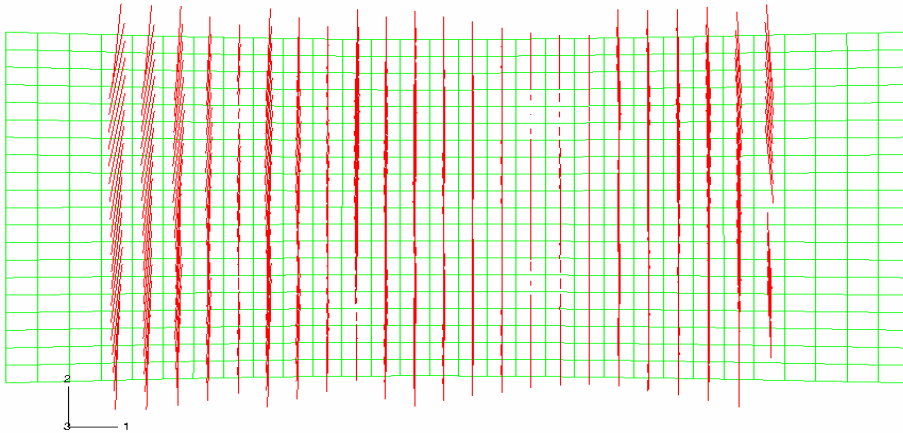


Figure11 Crack Pattern for, SNEG, SNEG, Load Step 17, Slab 355.6 mm., Voids 1.83 m.

Table 1. Deflection and Cracked Elements for Slab Thickness Variation

Slab Thickness (mm)	Deflection at Final Step (mm)	No. of rows of Cracked Element Rows	
		At Crack Initiation	At Final Step
304.8	13.97	7	23
355.6	12.45	5	22

Table 2. Deflection and Cracked elements for Voids up to 0.91 m.

Voids upto (m)	Slab Thickness (mm)	Deflection at Final Step (mm)	No. of rows of Cracked Element Rows	
			At Crack Initiation	At Final Step
0.91	304.8	14.48	7	24
0.91	355.6	12.70	5	23

Table 3. Deflection and Cracked Elements for Voids up to 1.83 m.

Voids upto (m)	Slab Thickness (mm)	Deflection at Final Step (mm)	No. of rows of Cracked Element Rows	
			At Crack Initiation	At Final Step
1.83	304.8	15.49	7	24
1.83	355.6	13.46	5	23